*J Mater Sci* (2017) 52:12370–12379

Energy materials

# Effect of expanded graphite and carbon nanotubes on the thermal performance of stearic acid phase change materials

Xiaomin Cheng[1,2], Ge Li[1,*], Guoming Yu[2], Yuanyuan Li[1], and Jiaqiang Han[1]

[1] School of Materials Science and Engineering, Wuhan University of Technology, Wuhan 430070, Hubei, China
[2] School of Mechanical and Electrical Engineering, Huanggang Normal University, Huanggang 438000, Hubei, China

**Received:** 12 February 2017
**Accepted:** 4 July 2017
**Published online:** 11 July 2017



## ABSTRACT

Carbon materials were added into stearic acid (SA) to improve the low thermal conductivity of SA, and their effect on thermal performance was investigated and compared. Stearic acid (SA)/expanded graphite (EG) and stearic acid (SA)/carbon nanotubes (CNTs) composite phase change materials (PCMs) were prepared via melt blending, vacuum adsorption and ultrasonication methods. Carbon additives were blended into SA with mass ratio from 1 to 9%. The leakage rate dropped dramatically with the increase in EG, and it was only physical adsorption in the preparation of both SA/EG and SA/CNTs composite PCMs. Thermophysical properties measured by TG-DSC showed that phase change temperatures of composite PCMs almost stayed the same and latent heat decreased slightly with increasing loadings of EG or CNTs. Thermal diffusivity and conductivity of pure SA were improved by adding EG and CNTs, while EG was far more effective than CNTs owing to the heat conduction network formed inside SA/EG composite PCMs, which was also the reason for the enhancement of thermal stability of SA/EG composite PCMs. Compared with pure SA, the thermal conductivity of composite PCMs was 6.2 times higher with 9 wt% EG and 1.4 times with 9 wt% CNTs, respectively. The heat storage and heat release efficiencies were also improved by carbon additives. This work demonstrates that EG is more potential to enhance the thermal performance of SA than CNTs, and SA/EG composite PCMs are quite promising for low-temperature solar energy storage.

## Introduction

Over the past several decades, an increasing concern over heavy emissions of greenhouse gas and limited reserves of fossil fuels makes the effective utilization of green energy a key issue. Solar energy, as a clean and renewable natural energy source, has become more and more commonly used. However, it exhibits significant instability and can be harvested only intermittently due to the influence of weather and

Address correspondence to E-mail: lige1018@whut.edu.cn



DOI 10.1007/s10853-017-1350-9

seasonal changes. To reduce the mismatch in the supply and demand of solar energy, PCMs (phase change materials) have been utilized as an effective method for solar energy storage. According to the types of phase change, PCMs can be classified as solid–solid, solid–liquid, solid–gas and liquid–gas PCMs. Among these, the solid–liquid PCMs are considered as a promising way to store thermal energy. Solid–liquid PCMs can store or release large amounts of thermal energy in the process of melting and solidifying. Additionally, variation of temperature, pressure and volume is small during the phase change process [1–3]. In particular, PCMs used for low-temperature latent heat energy storage (LHES) have attracted increasing attention and been widely applied in many energy storage and management fields, such as solar energy heating [4, 5], building energy efficiency [6–8], smart textiles [9, 10], electronics [11, 12], automotive [13, 14].

Among PCMs for low-temperature LHES, the interest in fatty acids ($CH_3(CH_2)_{2n}COOH$) has increased these years due to their high latent heat of fusion, reproducible melting and solidifying behavior with little or no supercooling, low cost, non-toxicity, good chemical and thermal stability [15]. Stearic acid has a more suitable phase change temperature for solar thermal energy storage systems than other fatty acids. However, SA has a low thermal conductivity like many other organic PCMs, and leakage is prone to occur when melting. These drawbacks have facilitated many studies about how to enhance the heat transfer and conductivity of PCMs in LHES, and prevent the leakage of PCMs when in the molten state, which have been realized by introducing materials with high thermal conductivity like metal particles, metal foams into PCMs, and encapsulating PCMs with $SiO_2$, PMMA in the core–shell structure. However, these improvement measures either increase the weight and cost of systems or decrease the latent heat of composite PCMs.

Carbon materials have excellent properties like high stability and thermal conductivity, low cost and density, which make them ideal thermal enhancement additives of PCMs to improve the thermal conductivity of PCMs with little loss of latent heat of fusion. Carbon additives in different sizes and morphologies have been widely investigated. Shi et al. [16] mixed multi-flake exfoliated graphite nanoplatelets (xGnP) and single-flake graphene into paraffin to study improvements in the thermal conductivity and shape stability of the matrix. The results show that there is a more than tenfold increase in thermal conductivity with a 10 wt% xGnP loading, and paraffin can maintain its shape up to 185.2 °C at a 2 wt% single-flake graphene loading. Zhong et al. [17] obtained a composite PCM consisting of a three-dimensional graphene aerogel (GA) and octadecanoic acid (OA). The thermal conductivity of the composite PCM was about 14 times than that of pure octadecanoic acid, while the high heat storage capacity was very close to the capacity of the acid. Form–stable composite PCMs prepared by vacuum impregnation of paraffin into graphene oxide (GO) sheets showed no leakage and greatly enhanced thermal conductivity from 0.305 to 0.985 W $(m\ K)^{-1}$ [18]. Cui et al. [19] studied thermal properties of carbon nanofiber (CNF) and carbon nanotube (CNT) filled phase change materials (soy wax and paraffin wax). The experiment was conducted by stirring CNF or CNT in liquid wax at 60 °C, and the results manifest that the thermal conductivity of composite PCMs increases as the increasing CNF or CNT loading contents. Tang et al. [20] added the tubular carbon nanotubes (CNTs) into the MA-SA eutectics to enhance the thermal conductivity. The supercooling degrees of obtained composite PCMs decrease obviously with an increase in the CNTs content, and the thermal conductivities of the composite PCMs increase significantly from 0.173 to 0.213, 0.258, 0.283 W $(m\ K)^{-1}$ as the mass fractions of the CNTs in the composite PCMs were 9, 12, 15 wt%. Additionally, the worm-like expanded graphite (EG) in a micrometer scale is commonly used to enhance thermal conductivity of PCMs and restrain leakage in the melting process simultaneously. Zhang et al. [21] prepared the CA–PA–SA ternary eutectic mixture firstly and mixed it with EG. The results show that the mass ratio of ternary eutectic mixture in composite PCMs can reach as high as 90% and thermal conductivity of composite PCMs is much higher than CA–PA–SA, thus obviously decreasing the melting and cooling time. Xia et al. [22] prepared expanded graphite/paraffin composite PCMs with mass fraction of EG varying from 0 to 10 wt%. An addition of 10 wt% EG can lead to a tenfold increase in the thermal conductivity compared to that of pure paraffin and reduce the heat storage/retrieval durations of EG(10)/paraffin(90) by 48.9 and 66.5%. Fang et al. [23] prepared SA/EG composites with mass ratios of 1:1, 3:1, 5:1, which exhibited the same phase

transition characteristics as SA, and their latent heats were consistent with values calculated based on the mass fraction of the stearic acid in the composites. Due to the adsorption ability of SA, there was no leakage of stearic acid even when composites were in the molten state.

Based on the literature described above and the fact that both micrometer-scale worm-like EG and nanometer-scale tubular CNTs are excellent thermal conductivity promoters among various carbon materials, there has been no comparative study about their thermal conductivity enhancement effects on stearic acid. Therefore, this study focuses on the comparison about structures and thermophysical properties of SA/EG and SA/CNTs composite PCMs. Samples with five different mass fractions of EG and CNTs were prepared by melt blending, vacuum adsorption and ultrasonication methods to study the effects of different amounts of carbon additives on the thermal performance of SA. The heat storage and release performance of SA, SA/EG and SA/CNTs composite PCMs were studied via a LHES system.

## Experimental

### Experimental materials

Stearic acid (Analytical Reagent, Sinopharm Chemical Reagent Co., Ltd, China) was used as matrix PCM without further purification. Expandable graphite (50 meshes, Qingdao Jinrilai Graphite Co., Ltd, China) was used to prepare expanded graphite (EG) via high-temperature expansion. Multi-wall carbon nanotubes (MWCNTs, >95 wt%, diameter 20–30 nm, length 10–30 μm) were purchased from Beijing Boyu Hi-Tech New Material Technology Co., Ltd, China.

### Preparation of SA/EG and SA/CNTs composite PCMs

EG was obtained by heating expandable graphite for 60 s in furnace set at 900 °C. The SA/EG composite PCMs were prepared by the following procedures: firstly, SA was heated for 20 min to melt completely in a water bath set at 80 °C; next, prepared EG was added into the molten SA to achieve different mass ratios of 1, 3, 5, 7, 9 wt%, and then the mixtures were stirred vigorously by a magnetic stirrer for 1 h, followed by a vacuum adsorption for 6 h in a vacuum oven set at 80 °C; Finally, the prepared samples were labeled as SA/EG-1, SA/EG-3, SA/EG-5, SA/EG-7, SA/EG-9. The SA/CNTs composite PCMs were prepared by following the same procedures, substituting EG for CNTs, vacuum adsorption for ultrasonication, and labeled as SA/CNTs-1, SA/CNTs-3, SA/CNTs-5, SA/CNTs-7, SA/CNTs-9. To test the packaging effect of EG, leakage tests were conducted via the method suggested by Yang et al. [24].

### Characterization

The phases of SA, EG, CNTs, and SA/EG-7, SA/CNTs-7 composite PCMs were characterized by X-ray diffraction (XRD, D8-ADVANCE, Bruker, Germany). The microstructures of EG, CNTs, and SA/EG-7, SA/CNTs-7 composite PCMs were observed by scanning electron microscope (SEM, S4800, Hitachi, Japan). The phase change temperatures, latent heats and thermal stability of SA and SA/EG-7, SA/CNTs-7 composite PCMs were achieved by thermogravimetric–differential scanning calorimetry (TG-DSC, STA449F3, Netzsch, Germany). The TG-DSC tests were carried out at 10 °C $min^{-1}$ under a constant stream of nitrogen. Thermal diffusivity and conductivity of SA, and SA/EG, SA/CNTs composite PCMs were obtained by Laser Flash Diffusivity Apparatus (LFA457, Netzsch, Germany). Tests of thermal diffusivity and conductivity were conducted three times for each sample in order to ensure reproducible data. Thermal energy storage performance test was conducted by inserting thermocouples into the tube filled with SA, SA/EG-7, SA/CNTs-7 composite PCMs, and heat storage and release curves were acquired by the data collected by a data logger. The temperature was controlled by a water bath at 80 °C for heat storage process and samples were cooled in the air to room temperature for heat release process.

## Results and discussions

### The optimal mass ratio of SA to EG

An ideal PCM should have an appropriate phase change temperature, a high thermal conductivity and latent heat, which means that EG should enhance the

thermal performance of SA and occupy relatively low content in composite PCMs for not losing much latent heat meanwhile. Furthermore, the adsorptive capacity of EG is limited; therefore, it is essential to determine the optimal mass ratio of SA to EG. Figure 1 and Table 1 show the weight loss and leakage rate of SA/EG composite PCMs during phase change based on leakage tests. The worm-like structure of EG can adsorb SA, and as the mass ratio of SA to EG increased from 1 to 9%, the leakage rate dropped dramatically, even down to 0.605% when mass ratio of EG to SA was 9%. Typically, it can be considered that SA can be packaged well by 7 wt% EG and SA/EG-7 composite PCMs has a relatively higher latent heat, which means 7% can be expected to be the optimal mass ratio of SA to EG. In the preparation of SA/CNTs composite PCMs, samples were in a liquid state similar to pure molten SA, which indicates CNTs can hardly adsorb SA. For the comparability between EG and CNTs, SA/EG-7 and SA/CNTs-7 composite PCMs are taken as subjects in the following discussion.

## Microstructure and phase analysis of EG, CNTs and composite PCMs

Figure 2a–d shows the morphologies of EG, CNTs, SA/EG-7 and SA/CNTs-7 composite PCMs, respectively. EG looks like silkworm larvae with the naked eye, and Fig. 2a shows that EG exhibits a porous structure which largely expands its specific surface area and can adsorb molten SA owing to capillary effect. It can be seen from Fig. 2c that SA fills in the porous network of EG, and layers of EG is completely covered with SA at an EG mass ratio of 7 wt%. Figure 2b shows that CNTs have curved tubular structures. Its diameter is about 30 nm and homogeneous, which is consistent with what is provided by the supplier. It can be seen from Fig. 2d that the surfaces and ends of CNTs are wrapped with SA, which seriously weakens the connection among CNTs to form an effective thermal conduction network. It can also be seen that CNTs is not uniformly distributed in SA.

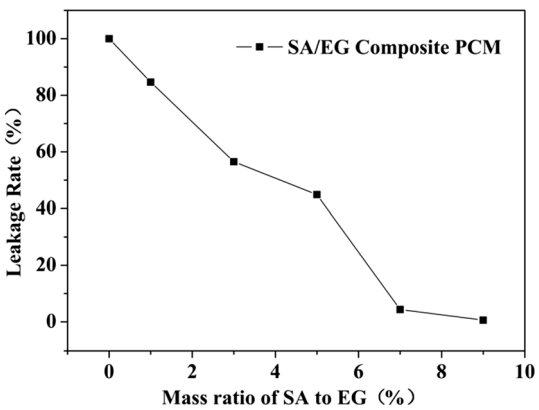


**Figure 1** Leakage rate of SA/EG composite PCMs.

The XRD patterns of SA, EG, CNTs, SA/EG-7, SA/CNTs-7 composite PCMs are depicted in Fig. 3. It can be seen from Fig. 3 that the diffraction peaks of SA lie at 6.8°, 11.2°, 21.6° and 24.2°. EG and CNTs exhibit a diffraction peak located at 26.5°, which is attributed to the characteristic peak of graphite (002). The diffraction peaks of SA/EG-7, SA/CNTs-7 composite PCMs lie at 6.8°, 11.2°, 21.6°, 24.2° and 26.5°, containing all characteristic peaks of SA and EG or SA and CNTs. Therefore, it is rather a physical combination than a chemical reaction in the preparation of composite PCMs which still maintain basic thermophysical properties of pure SA.

## Thermophysical properties of composite PCMs

The thermophysical properties of SA, SA/EG and SA/CNTs composite PCMs are listed in Tables 2 and 3, and the phase change temperature and latent heat comparisons of SA, SA/EG and SA/CNTs composite PCMs are shown in Fig. 4. It can be seen from Table 2 that the melting and solidifying temperatures of SA are 71.45 and 69.21 °C, respectively, which is suitable for low-temperature solar energy storage. The melting and solidifying latent heats of SA are 219.39 and 216.65 J $g^{-1}$, respectively, which are much higher latent heats than that of other PCMs and an important factor for thermal energy storage. In the melting process of both SA/EG and SA/CNTs composite PCMs, it can be seen from Fig. 4a that the onset temperature decreases a little compared with pure SA, which is mainly caused by the enhancement of thermal conductivity after adding carbon materials. High thermal conductivity contributes a lot to thermal conduction which plays a leading role in solid–liquid phase change. For the solidifying process, the onset temperature of SA/EG composite PCMs also decreases a little compared with pure SA shown in Fig. 4b. Given that EG has large specific surface area and capillary effect which can adsorb molten SA, the separated SA has a negative effect on convection

**Table 1** Mass ratio, weight and leakage rate of SA/EG samples before and after leakage test

| Samples | Mass ratio (SA:EG) | Weight before leakage test (g) | Weight after leakage test (g) | Leakage rate (%) |
|---|---|---|---|---|
| SA | 100:0 | 0.500 | 0 | 100 |
| SA/EG-1 | 99:1 | 0.500 | 0.077 | 84.6 |
| SA/EG-3 | 97:3 | 0.500 | 0.218 | 56.4 |
| SA/EG-5 | 95:5 | 0.500 | 0.276 | 44.8 |
| SA/EG-7 | 93:7 | 0.500 | 0.478 | 4.4 |
| SA/EG-9 | 91:9 | 0.500 | 0.497 | 0.6 |

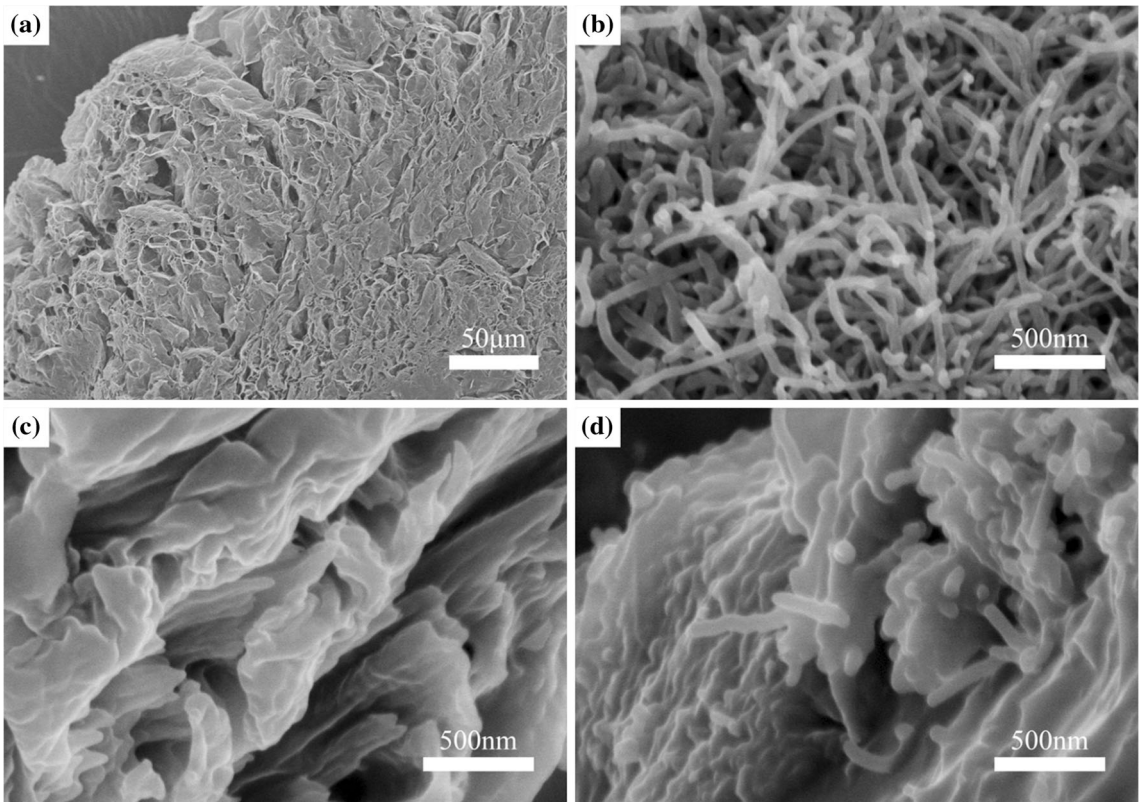


**Figure 2** SEM images of **a** EG, **b** CNTs, **c** SA/EG-7 and **d** SA/CNTs-7.

during liquid–solid phase transition. As is indicated by Fig. 4a, the onset temperature of SA/CNTs composite PCMs increases a little because of the enhancement of thermal conductivity when solidifying. It is evident from Fig. 4c, d that the latent heat of all SA/EG and SA/CNTs composite PCMs decreases with the increase in the content of carbon additives. Because carbon additives used for enhancing thermal conductivity and packaging do not absorb or release heat in the DSC test, the latent heat of composite PCMs is mainly contributed by SA. Under the circumstance that 7 wt% EG can package SA well, the latent heat of SA/EG-7 in melting and solidifying process is 198.34 and 198.83 J $g^{-1}$, respectively, while that of SA/CNTs-7 is 192.60 and 186.65 J $g^{-1}$, respectively. In general, the phase change temperature of composite PCMs stays almost the same and the latent heat of composite PCMs still remains high in spite of the addition of carbon materials.

From Table 4, it is evident that the thermal diffusivity and conductivity of SA/EG and SA/CNTs composite PCMs increase with the increasing mass ratio of carbon additives. The thermal diffusivity and conductivity of SA are 0.170 $mm^2 s^{-1}$ and 0.415 W $m^{-1} K^{-1}$, which curbs the application of SA in the field of thermal energy storage. After adding

EG into SA, the thermal diffusivity and conductivity of SA/EG-9 composite PCM can reach up to 3.860 $mm^2 s^{-1}$ and 2.556 $W m^{-1} K^{-1}$, which are higher than that of SA/CNTs-9 composite PCM and pure SA. The thermal diffusivity and conductivity of SA/CNTs-9 composite PCM are 0.203 $mm^2 s^{-1}$ and 0.593 $W m^{-1} K^{-1}$, which are little higher than pure SA. In general, the thermal diffusivity and conductivity of SA/EG composite PCMs are much higher than those of SA/CNTs composite PCM with the same mass ratio of carbon additives. It can be easily seen from Table 4 that EG has a greater ability to improve the thermal diffusivity and conductivity of SA than CNTs, which is in agreement with microstructures of EG and CNTs. Carbon layers of EG are derived from individual expandable graphite treated with high-temperature expansion, as a result, they are connected with each other inside which is beneficial to form effective heat conduction network. However, the nanoscale tubular structure of CNTs is not apt to form effective heat conduction network based on point–point contact as shown in the SEM image of SA/CNTs-7 composite PCM. Furthermore, uneven distribution and aggregation caused by nanoscale effect also have a negative effect on the enhancement of thermal diffusivity and conductivity.

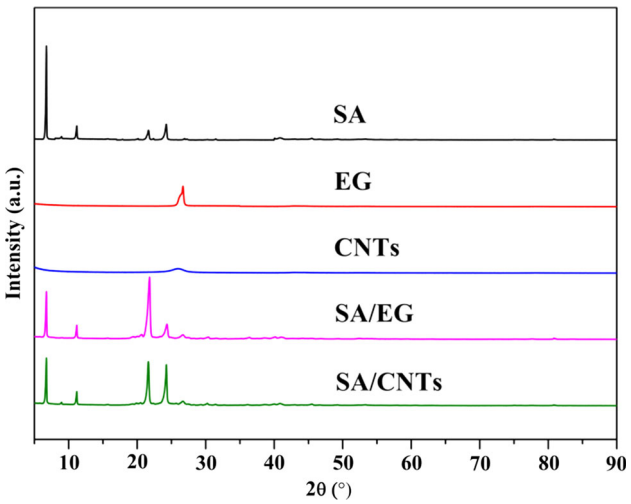


**Figure 3** XRD patterns of SA, EG, CNTs, SA/EG-7, SA/CNTs-7 composite PCMs.

## Thermal stability of composite PCMs

Figure 5 indicates the TG and DTG curves of SA, SA/EG-7, SA/CNTs-7 composite PCMs. It can be seen from Fig. 5 that the onset temperature ($T_{onset}$), the 5% weight loss temperature ($T_{5\%}$) and the maximum weight loss rate ($T_{max}$) of SA/EG-7 are 303, 274 and 332 °C, respectively, which are higher than those of pure SA (292, 262 and 320 °C, respectively). However, $T_{onset}$, $T_{5\%}$ and $T_{max}$ of SA/CNTs-7 (291, 264, 319 °C) stay almost the same with pure SA. This

**Table 2** DSC data of SA and SA/EG composite PCMs

| Samples | Melting | | Solidifying | |
|---|---|---|---|---|
| | Onset temperature/ °C | Latent heat/J $g^{-1}$ | Onset temperature/ °C | Latent heat/J $g^{-1}$ |
| SA | 71.45 | 219.39 | 69.21 | 216.65 |
| SA/EG-1 | 70.94 | 214.22 | 69.24 | 214.92 |
| SA/EG-3 | 71.11 | 203.13 | 68.89 | 203.96 |
| SA/EG-5 | 70.87 | 202.02 | 68.93 | 202.92 |
| SA/EG-7 | 70.80 | 198.34 | 68.73 | 198.83 |
| SA/EG-9 | 70.79 | 191.93 | 68.41 | 194.76 |

**Table 3** DSC data of SA and SA/CNTs composite PCMs

| Samples | Melting | | Solidifying | |
|---|---|---|---|---|
| | Onset temperature/ °C | Latent heat/J $g^{-1}$ | Onset temperature/ °C | Latent heat/J $g^{-1}$ |
| SA | 71.45 | 219.39 | 69.21 | 216.65 |
| SA/CNTs-1 | 71.06 | 210.51 | 69.94 | 206.62 |
| SA/CNTs-3 | 70.91 | 204.84 | 69.94 | 205.02 |
| SA/CNTs-5 | 71.01 | 195.09 | 69.92 | 190.39 |
| SA/CNTs-7 | 70.80 | 192.60 | 69.57 | 186.65 |
| SA/CNTs-9 | 70.64 | 178.49 | 69.54 | 175.54 |

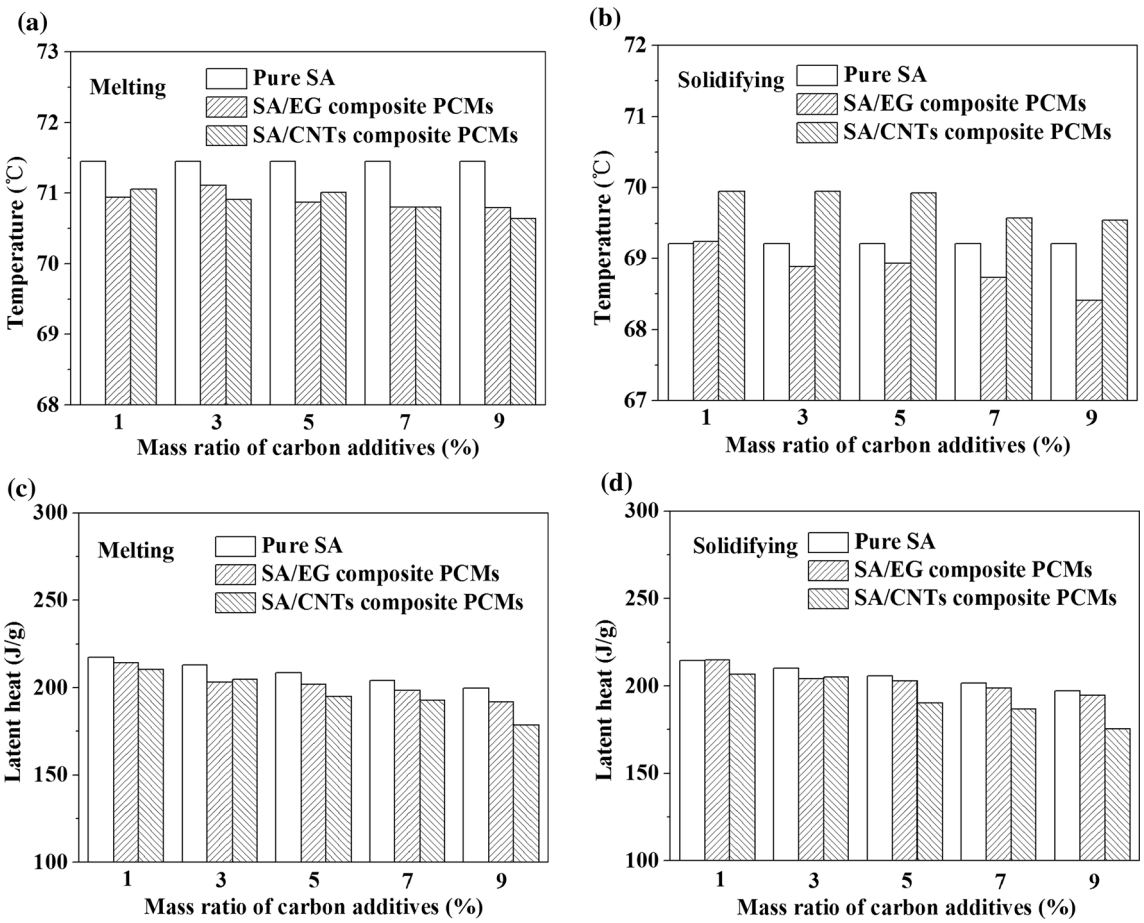


**Figure 4** **a** Melting temperature, **b** solidifying temperature, **c** melting latent heat and **d** solidifying latent heat of SA, SA/EG, SA/CNTs composite PCMs.

**Table 4** Thermal diffusivity and conductivity of SA, SA/EG and SA/CNTs composite PCMs

| Samples | Thermal diffusivity ($mm^2\ s^{-1}$) | Thermal conductivity ($W\ m^{-1}\ K^{-1}$) |
|---|---|---|
| SA | 0.170 | 0.415 |
| SA/EG-1 | 0.265 | 0.472 |
| SA/EG-3 | 0.750 | 0.698 |
| SA/EG-5 | 1.047 | 0.742 |
| SA/EG-7 | 3.196 | 2.191 |
| SA/EG-9 | 3.860 | 2.556 |
| SA/CNTs-1 | 0.172 | 0.420 |
| SA/CNTs-3 | 0.177 | 0.430 |
| SA/CNTs-5 | 0.179 | 0.472 |
| SA/CNTs-7 | 0.191 | 0.519 |
| SA/CNTs-9 | 0.203 | 0.593 |

manifests that adding EG can enhance the thermal stability and extend the operating temperature of pure SA because of the adsorption capacity of EG which is not possessed by CNTs, and that is the reason why the addition of CNTs cannot improve the thermal stability of SA.

## Heat storage and release performance of SA, SA/EG-7, SA/CNTs-7 composite PCMs

Good thermal performance of PCM during heat storage and release process is very important for thermal energy storage systems. Figure 6 shows the

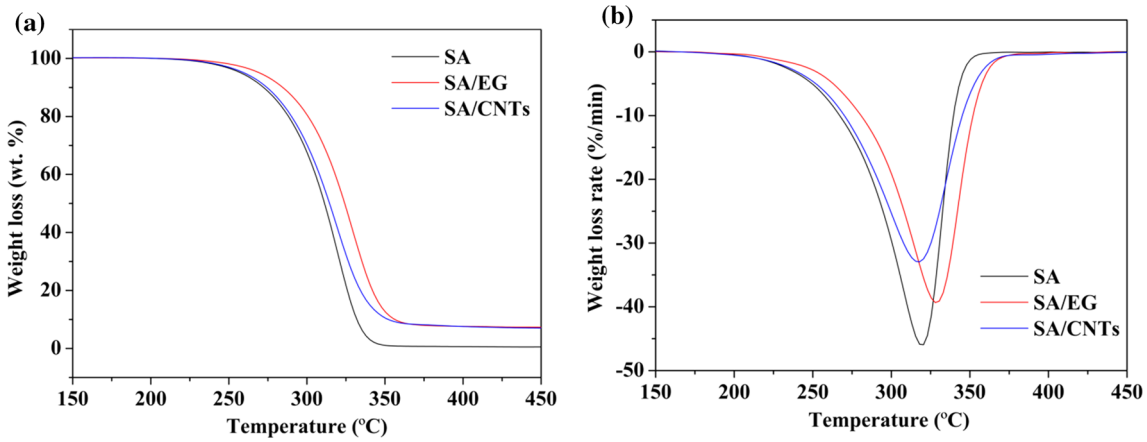


**Figure 5** **a** TG curves and **b** DTG curves of SA, SA/EG, SA/CNTs composite PCMs.

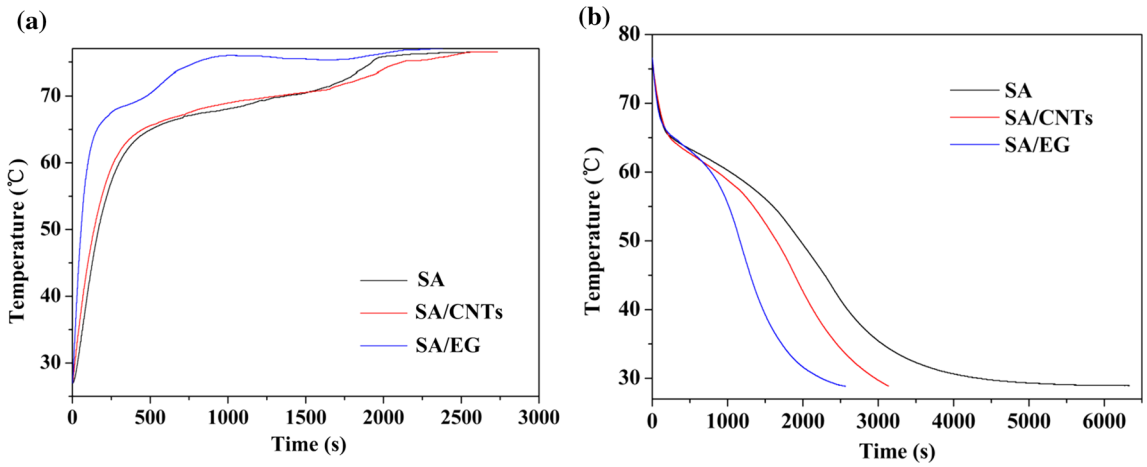


**Figure 6** Temperature changes in heat **a** storage and **b** release process of SA, SA/EG-7, SA/CNTs-7 composite PCMs.

heat storage and release curves of SA, SA/EG-7 and SA/CNTs-7 composite PCMs. It can be seen from Fig. 6 that it takes 473 s with SA/EG-7, 1299 s with SA/CNTs-7 and 1362 s with SA to reach the melting temperature at 70 °C, and the time for heat release is 2564 s with SA/EG-7, 3139 s with SA/CNTs-7 and 6331 s with SA. Compared with pure SA, the time needed for heat storage and release with SA/EG-7 composite PCM is reduced by 65.3 and 59.5%, respectively, while the time for SA/CNTs-7 composite PCM only decreases by 4.6 and 50.4%, correspondingly. This indicates that a complete cycle of heat storage and release decreases by adding carbon materials like EG and CNTs, which can be explained by the thermal conductivity enhancement of SA/EG-7 and SA/CNTs-7 composite PCMs compared with pure SA. In both heat storage and release process, high thermal conductivity contributes a lot in increasing the efficiency of heat transfer, so SA/EG-7 composite PCM performs best. On account of low thermal conductivity of SA/CNTs-7 composite PCM, SA/CNTs-7 almost performs the same with pure SA in heat storage process, while good convection enables the heat transfer efficiency of SA/CNTs-7 to lie between that of SA/EG-7 and SA in heat release process.

## Conclusions

This paper aims to study the effects of micrometer-scale worm-like EG and nanometer-scale tubular CNTs on SA and compare the difference in structures and thermophysical properties of SA/EG and SA/CNTs composite PCMs. The XRD results show that it is only a physical combination in the preparation of SA/EG and SA/CNTs composite PCMs. The leakage test shows that 7% is the optimal mass ratio of SA to

EG, and SEM images indicate that 7 wt% EG is completely covered by SA and layers of EG are connected with each other to form effective conduction network. However, CNTs is not uniformly distributed in SA from SEM image and point–point contact is not beneficial for heat transfer. The DSC results manifest that the melting and solidifying temperatures of composite PCMs are approximately 71 and 69 °C, respectively, and the latent heats of them decrease with the increase in the mass fraction of carbon additives. The thermal diffusivity and conductivity results show that EG is more effective than CNTs in enhancing the performance of heat transfer because of its effective conduction network formed inside SA/EG composite PCMs. There is a 6.2-fold increase in the thermal conductivity with an addition of 9 wt% EG, while the 9 wt% CNTs increase the thermal conductivity by a factor of 1.4. The TG and DTG results indicate that SA/EG composite PCM exhibits better thermal stability than SA/CNTs composite PCM. The heat storage and release test of SA, SA/EG and SA/CNTs composite PCMs in a LHES system reveals that the time required for heat storage and release is reduced more by EG than CNTs due to the high thermal conductivity of SA/EG composite PCM. All the results demonstrate that thermophysical properties of SA can be improved by adding EG and CNTs, while EG has greater potential to enhance the thermal performance than CNTs. The prepared composite PCMs are quite promising in the application for low-temperature solar energy storage.

## Acknowledgements

This work was supported by the National Key Technology Research & Development Program of China (Grant No. 2012BAA05B05, Ministry of Science and Technology of the People's Republic of China), Key Technology Research & Development Program of Hubei (Grant No. 2015BAA111, Science and Technology Department of Hubei Province) and the Fundamental Research Funds for the Central Universities (Grant No. WUT2017II23GX, Wuhan University of Technology).

## Compliance with ethical standards

**Conflicts of interest** All authors declare no conflict of interest.

## References

[1] Pielichowska K, Pielichowski K (2014) Phase change materials for thermal energy storage. Prog Mater Sci 65:67–123

[2] Sharma A, Tyagi VV, Chen CR et al (2009) Review on thermal energy storage with phase change materials and applications. Renew Syst Energy Rev 13:318–345

[3] Liu C, Li F, Ma L et al (2010) Advanced materials for energy storage. Adv Mater 22:28–62

[4] Shukla A, Buddhi D, Sawhney RL (2009) Solar water heaters with phase change material thermal energy storage medium: a review. Renew Syst Energy Rev 13:2119–2125

[5] Kant K, Shukla A, Sharma A et al (2016) Thermal energy storage based solar drying systems: a review. Innov Food Sci Emerg 34:86–99

[6] Iten M, Liu S, Shukla A (2016) A review on the air-PCM-TES application for free cooling and heating in the buildings. Renew Syst Energy Rev 61:175–186

[7] He Y, Zhang X, Zhang Y et al (2016) Utilization of lauric acid-myristic acid/expanded graphite phase change materials to improve thermal properties of cement mortar. Energy Build 133:547–558

[8] Pomianowski M, Heiselberg P, Zhang Y (2013) Review of thermal energy storage technologies based on PCM application in buildings. Energy Build 67:56–69

[9] Sarier N, Onder E (2012) Organic phase change materials and their textile applications: an overview. Thermochim Acta 540:7–60

[10] Mondal S (2008) Phase change materials for smart textiles—an overview. Appl Therm Eng 28:1536–1550

[11] Shaikh S, Lafdi K (2010) C/C composite, carbon nanotube and paraffin wax hybrid systems for the thermal control of pulsed power in electronics. Carbon 48:813–824

[12] Ling Z, Wang F, Fang X et al (2015) A hybrid thermal management system for lithium ion batteries combining phase change materials with forced-air cooling. Appl Energy 148:403–409

[13] Javani N, Dincer I, Naterer GF (2014) New latent heat storage system with nanoparticles for thermal management of electric vehicles. J Power Sources 268:718–727

[14] Lin C, Xu S, Chang G et al (2015) Experiment and simulation of a LiFePO4 battery pack with a passive thermal management system using composite phase change material and graphite sheets. J Power Sources 275:742–749

[15] Yuan Y, Zhang N, Tao W et al (2014) Fatty acids as phase change materials: a review. Renew Syst Energy Rev 29:482–498

[16] Shi J, Ger M, Liu Y et al (2013) Improving the thermal conductivity and shape-stabilization of phase change materials using nanographite additives. Carbon 51:365–372

[17] Zhong Y, Zhou M, Huang F et al (2013) Effect of graphene aerogel on thermal behavior of phase change materials for thermal management. Sol Energy Mater Sol C 113:195–200

[18] Mehrali M, Latibari ST, Mehrali M et al (2013) Shape-stabilized phase change materials with high thermal conductivity based on paraffin/graphene oxide composite. Energy Convers Manag 67:275–282

[19] Cui Y, Liu C, Hu S et al (2011) The experimental exploration of carbon nanofiber and carbon nanotube additives on thermal behavior of phase change materials. Sol Energy Mater Sol C 95:1208–1212

[20] Tang Y, Alva G, Huang X et al (2016) Thermal properties and morphologies of MA–SA eutectics/CNTs as composite PCMs in thermal energy storage. Energy Build 127:603–610

[21] Zhang H, Gao X, Chen C et al (2016) A capric–palmitic–stearic acid ternary eutectic mixture/expanded graphite composite phase change material for thermal energy storage. Compos Part A Appl S 87:138–145

[22] Xia L, Zhang P, Wang RZ (2010) Preparation and thermal characterization of expanded graphite/paraffin composite phase change material. Carbon 48:2538–2548

[23] Fang G, Li H, Chen Z et al (2010) Preparation and characterization of stearic acid/expanded graphite composites as thermal energy storage materials. Energy 35:4622–4626

[24] Yang X, Yuan Y, Zhang N et al (2014) Preparation and properties of myristic–palmitic–stearic acid/expanded graphite composites as phase change materials for energy storage. Sol Energy 99:259–266